

## **NUMERICAL ANALYSIS OF A SANDWICH COMPOSITE USING OPEN FOAM SOFTWARE**

**ANDRÉ C. GARAY<sup>1</sup>, MATHEUS FRANZ<sup>2</sup>, JEFERSON A. SOUZA<sup>2</sup>  
and SANDRO C. AMICO<sup>1</sup>**

<sup>1</sup>PPGEM

Federal University of Rio Grande do Sul (FURGS)  
P.O. Box 15010, 91501-970  
Porto Alegre/RS  
Brazil

<sup>2</sup>School of Engineering

Federal University of Rio Grande (FURG)  
Av. Itália, Km 08 s/n  
Campus Carreiros  
96203-900, Rio Grande/RS  
Brazil  
e-mail: jasouza@furg.br

### **Abstract**

Resin Transfer Molding (RTM) and its variant, Light resin transfer molding (LRTM) are liquid composite processes largely used in manufacturing pieces with high mechanical properties and good finishing in both sides. In these processes, a polymeric resin is injected into a mold cavity previously filled with a reinforced media. Besides the reinforced media, and when light pieces are necessary, an impermeable material is placed at the core section of the assemble. The final sandwich piece is a composite compound by a polymeric matrix, a fibrous reinforced media and a light non permeable core. Good mechanical properties associated with a low density composite are the desired characteristics of this structure. In this work, numerical modelling of the resin advance through the porous reinforced media has been used to predict filling

---

Keywords and phrases: RTM, numerical model, sandwich composite.

Received May 31, 2015

time and void formation in a sandwich composite piece. The pieces are manufactured with the LRTM process on which a lateral empty (without reinforcement) border is used to inject the resin. In the LRTM process, the computational domain is divided in two regions: A porous (with reinforcement) and the empty channel. The volume of fluid (VOF) method was used to solve the fluid mechanical problem in both domains. Results have shown that the proposed methodology is capable of predicting flow advance inside the mold, however the solution is highly dependent on the physical properties of the reinforcement, mainly the permeability. Case studies are presented for different operating conditions.

## 1. Introduction

Resin transfer molding (RTM) is a liquid molding process largely used in automotive, naval and more recently, aerospace industry. In the RTM, a polymeric resin is forced to flow inside a mold cavity filled with a porous reinforced media. Manufacturing is completed with the cure process, which occurs right after molding injection. Complex pieces with good mechanical properties and good finishing in both sides are easily produced with this process. When light pieces are desired, it is possible to build low weight composites by the addition of an impermeable core to the reinforced media, producing a lighter piece that stills having good mechanical properties.

A variant of the traditional RTM, the Light RTM (LRTM), brings two advantages to the manufacturing process: Composite molds (less expensive) can be used and fast injection is obtained. In this process, resin flows first through an empty (without reinforced media) lateral channel that surrounds the mold cavity and then starts to flow from the borders toward to the center. Outlet section is usually positioned at the geometric center of the piece. Process drawbacks are the fact that only low pressures can be used and piece thickness usually present undesired variations.

In these processes, numerical modelling of resin advance inside mold cavity plays an important role in mold design and injection problems prediction. Many methods have been proposed to simulate the resin flow

advance ([1], [2], [3]), however the two most used methodologies are the finite element-control volume (FE-CV) [4], and the volume of fluid (VOF) [5].

Development of FE-CV and VOF methodologies applied to RTM problems have been study by several authors. Studies include edge effect [6], new methods [7], void formation [8], among many others.

Other works have concentrated their enforces to improve the capability of the methods in detecting dry spots (voids) inside the composite ([8], [9], [10]). With the VOF method, void formation is automatically detect, however this method is much more time consuming and have some convergence problems. The FE-CV methods are faster and much more stable in terms of convergence, however dry spots can not be predicted without the use of a specific formulation.

In other to predict the injection with good agreement in terms of filling time, physical properties of resin and reinforced media need to be precisely determined. In most cases, experimental runs are used to permeability determination, however a few works uses a combination of experimental data with numerical solution in order to calculate media permeability. Some examples are given by [11] and [12].

In terms of RTM mold design, one of the most common problems in RTM is related to the positioning of injection and outlet ports. Related to this issue, numerical mold is an important tool to reduce costs and time in mold design ([13], [14]).

Finally, there are applied studies that concentrate in study a specific engineering problem and propose and efficient solution in terms of process operation, mold design or final piece quality. Examples are [14], [15], and [16].

In this work, it is presented a study about the use of numerical modelling to predict injection problems in a sandwich piece. Numerical and experimental solutions are compared in order to validate the numerical approach and 3 possible situations are numerical simulated in order to predict resin behaviour during the injection process.

## 2. Problem Description

A sandwich part is assembled with a impermeable core covered by a composite structure made with resin and fabric. RTM-Light process is used to infiltrate resin into a reinforced media previously placed in the mold cavity.

### 2.1. Geometry and computational domain

Figure 1 shows the problem geometry. Reinforced media is represented by the green part while the lateral injection channels, together with the tubes that connects upper and lower reinforced sheets are showed in orange. The space between the two reinforced plates is filled with a non permeable material (not shown in Figure 1). Inlet and outlet ports are also presented in Figure 1.

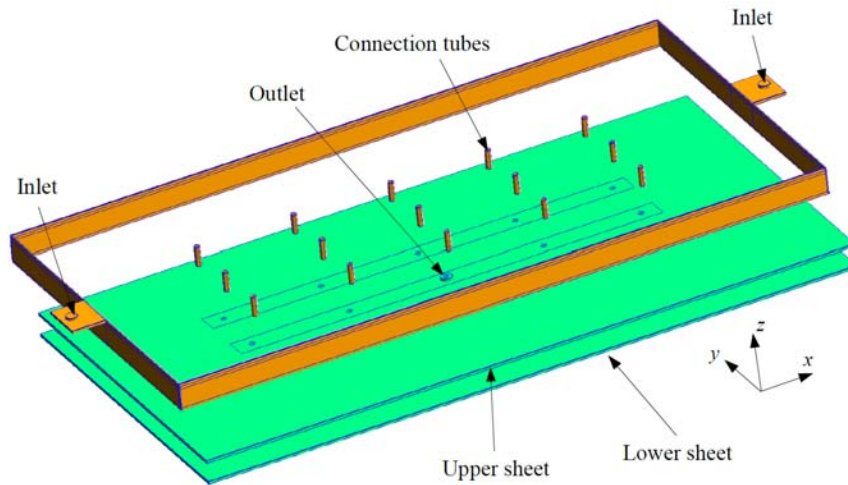


**Figure 1.** Geometry of the sandwich part.

Problem geometry shown in Figure 1 is a representation of the real mold which was build in a composite material. The injection channel was drawn with several rectangles, however in the real geometry these channels are irregular, i.e., the geometry presented in Figure 1 is a idealized representation of the constructed model. The geometry has

0.6m, 0.3m, and 0.025m in the  $x$ ,  $y$ , and  $z$  directions, respectively, inlet and outlet diameters of 0.005m and connection tubes with diameter equal to 0.0025m.

The geometry is simple, however there is a large size difference between the major faces (side, bottom, and up), and the diameter of the tubes connecting the upper and lower sheets. This non-uniformity brings no problems for the geometry creation, but forces a large number of elements in the discretization. The grid was made uniform where ever possible and hexahedra elements were used in creation of the lateral injection channels (outside orange parts in Figure 1), and the reinforced media (green in Figure 1) was created with prismatic elements. The computational domain was discretized with about 43,000 hexahedra (6 faces) and 280,000 prisms (5 faces).

Geometry and discretion where performed with GMSH [17] software. In Figure 2 is shown details of the inlet and outlet sections, respectively.

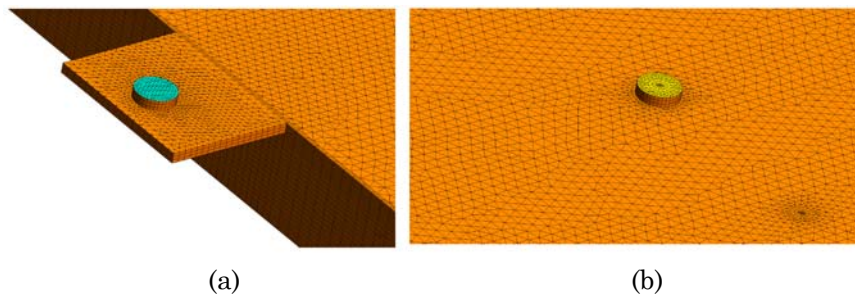


**Figure 2.** Geometry discretization: (a) inlet section and (b) outlet section.

## 2.2. Mathematical formulation

OpenFOAM software [18] has been used to solve the resin flow advance problem inside the mold. OpenFOAM uses the VOF (volume of fluid) [5] to solve multiphase problems with two or more immiscible fluids. In current solution, the phases are resin and air. This formulation considers all phases well defined and the volume occupied by one phase can not be occupied by the other phase. In this method, a volume fraction function,  $\alpha$ , is defined such as:

- (i) If  $\alpha = 0$  the cell is full with air.
- (ii) If  $\alpha = 1$  the cell is full with resin.
- (iii) If  $0 < \alpha < 1$  the cell contains the interface between phases air and resin.

Fluid flow problem is solve with only one set of momentum equations. Same velocity and pressure fields are used for both fluids, and the volume fraction calculated for every computational grid cell (control volume) is tracked throughout the domain by the addition of a transport equation for  $\alpha$ . The formulation for an incompressible flow is composed by the continuity, momentum and volume fraction equations (Equations (1), (2), and (7)).

The continuity equation is given by

$$\nabla \cdot (\vec{V}) = 0, \quad (1)$$

where  $\vec{V}$  is the velocity vector [m/s].

The momentum equation is given by

$$\frac{\partial(\rho\vec{V})}{\partial t} + \nabla \cdot (\rho\vec{V}\vec{V}) = -\nabla p + \nabla \cdot (\mu\overline{\overline{\tau}}) + \rho\vec{g} + \vec{F} + \sigma\kappa\nabla\alpha, \quad (2)$$

where  $\rho$  is the density [kg/m<sup>3</sup>],  $\mu$  is the absolute viscosity [Pa s],  $p$  is a pseudo-dynamic pressure [Pa],  $\vec{g}$  is the gravity vector [m/s<sup>2</sup>], and  $\overline{\overline{\tau}}$  is the stress tensor [Pa].

Term  $\vec{F}$  in Equation (2) is used to model the flow resistance imposed by the reinforced media. From Darcy's law, it is possible to correlate velocity and pressure drop such as

$$\vec{F} = \nabla p = -\frac{\mu}{\overline{\overline{K}}}\vec{V}, \quad (3)$$

where  $\overline{\overline{K}}$  is the permeability tensor [m<sup>2</sup>].

Physical properties are average among phases by the volume fraction as [19]

$$\rho = \alpha\rho_{\text{resin}} + (1 - \alpha)\rho_{\text{air}}, \quad (4)$$

$$\mu = \alpha\mu_{\text{resin}} + (1 - \alpha)\mu_{\text{air}}. \quad (5)$$

Last term on right in Equation (2) considers the effect of the surface tension. In this term,  $\sigma$  is the surface tension coefficient [N/m] and  $\kappa$  is the curvature of the interface calculated as [20]

$$\kappa = \frac{\nabla\alpha}{|\nabla\alpha|}. \quad (6)$$

The volume fraction equation is given by

$$\frac{\partial\alpha}{\partial t} + \nabla \cdot (\alpha\vec{V}) + \nabla \cdot \vec{V}_c\alpha(1 - \alpha) = 0, \quad (7)$$

where  $|V_c| = \min[c_\alpha|\vec{V}|, \max|\vec{V}|]$  and  $c_\alpha$ , a factor to be specified by the user.

The last term on right of Equation (7) is defined as the artificial compression and is used to guarantee physical results at the interface of the fluids [20].

### 2.3. Numerical modelling

According to Figure 1, the following boundary conditions were set:

- **Inlet:** Prescribed pressure  $P_0$  and prescribe volume fraction  $\alpha = 1$ .
- **Outlet:** Prescribed pressure equal to zero (gauge) and zero gradient for  $\alpha$ .
- **Walls:** Prescribed velocity equal zero and zero gradient for  $\alpha$ .

The initial conditions in all computational domain for volume fraction and velocity fields were set to zero.

Several cases have been simulated with small differences in boundary condition and geometry, however the basic physical properties and operating conditions are shown in Table 1.

**Table 1.** Physical properties and operating conditions

|                | Symbol                       | Value                 | Dimension           |
|----------------|------------------------------|-----------------------|---------------------|
| Courant number | $Co = V \Delta t / \Delta x$ | 0.5                   | –                   |
| Inlet pressure | $P_0$                        | 0.7                   | bar                 |
| Density        | $\rho$                       | 919                   | kg / m <sup>3</sup> |
| Viscosity      | $\mu$                        | 0.065                 | Pa s                |
| Porosity       | $\varepsilon$                | 0.85                  | –                   |
| Permeability   | $K$                          | $1.83 \times 10^{-9}$ | m <sup>2</sup>      |

With the parameters set as in Table 1, each simulation has a filling time of approximated 15 min and takes about 4 days running in parallel (four cores) in an Intel(R), Xeon(R) CPU E31240 @ 3.30GHz workstation under CentOS linux operating system.

OpenFOAM uses the finite volume method to discretize the conservation equations. As shown in Subsection 2.1, the diameter of the connection tubes is 240 times smaller than the mold length in  $x$  direction, thus the grid shown in Figure 2 is considerably refined and solution independence to space and time discretizations was insured by keeping the Courant number at a low value as shown in Table 1. Maximum Courant number recommended for the interFoam solver is 0.5 at fluid interface and 1 in all others regions. In current simulation, Courant number was kept at 0.5 in all computational domain. As grid elements are constant, time step is set to  $1 \times 10^{-8}$  s at the beginning and let free to vary during simulation in order to guarantee  $Co \leq 0.5$ . Usually, maximum time step reached was of  $1 \times 10^{-4}$  s, however in order to avoid possible solution problems, maximum time step was set to  $1 \times 10^{-3}$  s.



Most of the solver control parameters were kept constant, however some of them have being chanced to facilitate the convergence. The modified parameters and other important sets are shown in Table 2.

**Table 2.** Physical properties and operating conditions

| Variable                     | Parameter                             |
|------------------------------|---------------------------------------|
| <b>Algorithm</b>             | <i>PIMPLE</i>                         |
| <b>Solvers</b>               |                                       |
| Velocity                     | <i>PBiCG</i>                          |
| Pressure                     | <i>PCG</i>                            |
| <b>Interpolation schemes</b> |                                       |
| Transient                    | <i>Euler</i>                          |
| Gradients                    | <i>CellMDLimited Gauss linear 1.0</i> |
| Divergent                    |                                       |
| div(phi_r, alpha)            | <i>Gauss interfaceCompression</i>     |
| div(rho*phi, U)              | <i>Gauss upwind</i>                   |
| div(phi, alpha)              | <i>Gauss upwind</i>                   |

#### 2.4. Experimental set up

The mold used in all experimental runs is shown in Figure 3. It was built in composite material by manual lamination with glass fiber and polyester resin. Mold cavity produces a rectangular sheet with dimensions of  $620 \times 310 \times 16$ mm.

Before injection, mold preparation include the following steps:

(i) Mold cleaning to avoid possible imperfections to the produced piece.

(ii) A layer of demoulding is applied to both mold and counter mold (Figure 3(a)).

(iii) Reinforced media (fabric) is homogeneously positioned inside the mold cavity (Figure 3(b)).

(iv) The impermeable core is placed above the first reinforced layer (Figure 3(c)).

(v) Another layer of reinforcement is positioned over the impermeable core (Figure 3(d)).

(vi) Mold and counter mold are assembled (Figures 3(a) and 3(f)).

Mold closing is done with vacuum. Positive pressure is set at injection point while vacuum is imposed at the vents. Positive pressure is imposed during injection only, while vacuum at the vents is kept until the end of resin cure.

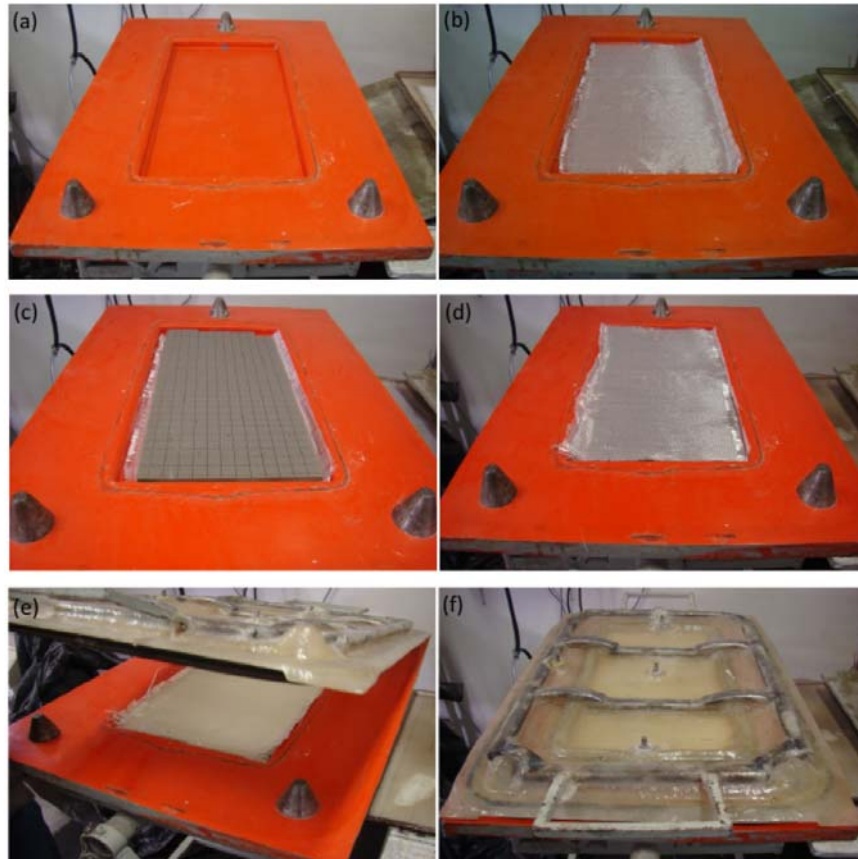


**Figure 3.** Mold assemble: (a) mold with demoulding; (b) lower layer of reinforced media; (c) impermeable composite core; (d) upper layer of reinforced media; (e) mold closing; and (f) mold closed for injection.

### 3. Results

In LRTM, the empty (no reinforcement) lateral channel makes resin to flow first through this channel, and than to converge into a vacuum point forming a circular like flow front as shown in Figure 5.

Numerical to experimental comparison was performed not by injecting a polymeric resin, which is expensive and more difficult to control the process parameters, but with a soyabean oil (properties are shown in Table 1), which is less expensive and simple to manipulate. Figure 4 shows results for resin position at different filling times. In Figure 4(a) (at 1s), the fluid has not come across the channel, while in Figure 4(b) (at 3s) resin has already filled the lateral channel and starts to enter the reinforced medium. In the experimental injection resin flow advance is not perfectly radial and converging to the center. This behaviour is due to the imperfections (heterogeneity) in the mold geometry (lateral channels mainly) an in the fibrous medium, making impossible to have a symmetric flow. In the experimental run, the mold was completed filled in 18s.

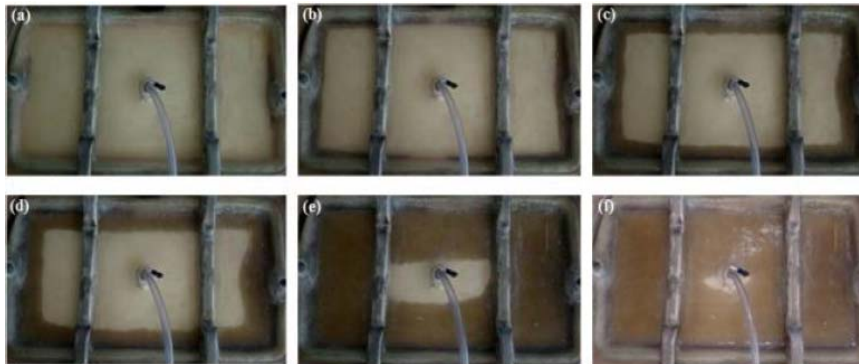


**Figure 4.** Experimental profile infiltration for different filling times: (a) 1s; (b) 3s; (c) 5s; (d) 10s; (e) 15s; and (f) 18s.

Geometry and process operating conditions of the experimental run showed in Figure 4 were than numerically simulated. In this solution, the total molding time was 14.8s, which is about 18% smaller than the

experimental filling time. Main difference between experimental and numerical solutions occurs at the beginning of the injection. For time equal to 1s, in the numerical simulation resin is already entering the fibrous medium while in the experimental run resin starts to come across the porous media only after 3s of injection.

Difference between numerical and experimental results may be explained by:

(i) Non-heterogeneity in experimental fiber physical properties (porosity and permeability). It is important to highlight that media permeability, which is a function of fabric positioning inside the mold and compression of the fibers, was obtained in a different experiment with a rigid (metallic) mold.

(ii) In the experimental run, the inlet pressure at the first moments of the injection is not constant, however it is considered constant in the numerical simulation.

(iii) The geometry of the lateral channel in the experimental mold is irregular and in some parts differs considerably from the virtual geometry.

Even with the differences discussed above, it is possible to perform a qualitative comparison between numerical and experimental solutions. The total filling time agrees in order of magnitude however flow front position differs if Figures 4 and 5 are compared. The border to center profile is observed in both numerical and experimental solutions, however in the numerical solution, resin starts to penetrate the reinforced media even before the lateral channels become completely filled. As expected, perfect symmetric profiles are obtained in the numerical solution.

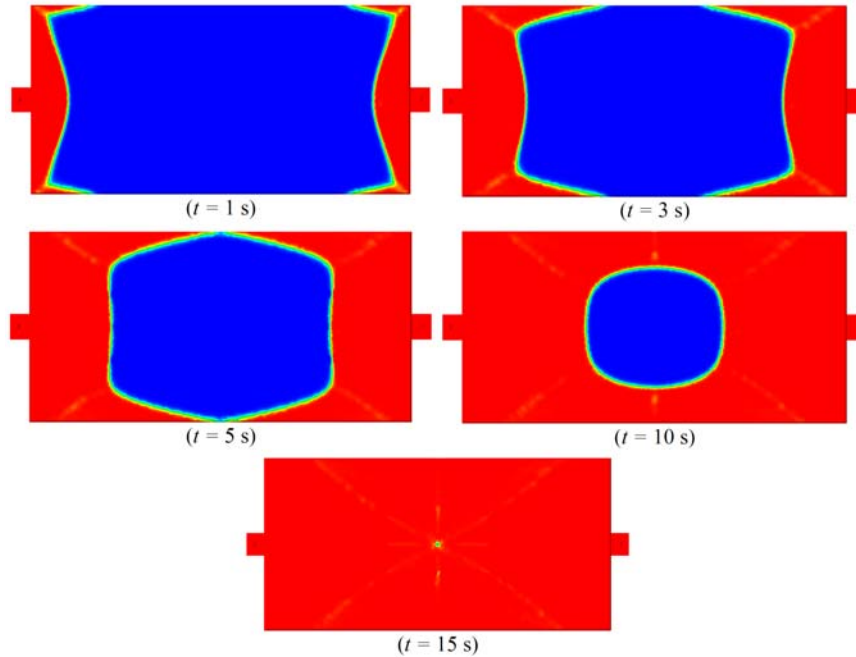


**Figure 5.** Numerical profile infiltration for different filling times.

The experimental mold was built with only one outlet positioned at the middle section of the upper reinforced media sheet. Thus, it was necessary to drill holes in the impermeable core allowing the air to flow from the lower sheet to the upper sheet and leave the mold through the outlet section. This holes are shown in a cut along the major symmetry axes of Figure 6.

In Figure 6, it can be seen that resin flows inside both upper and lower sheets at the same velocity. At the end of the simulation (15s), air bobbles can be visualized inside the connecting tubes.

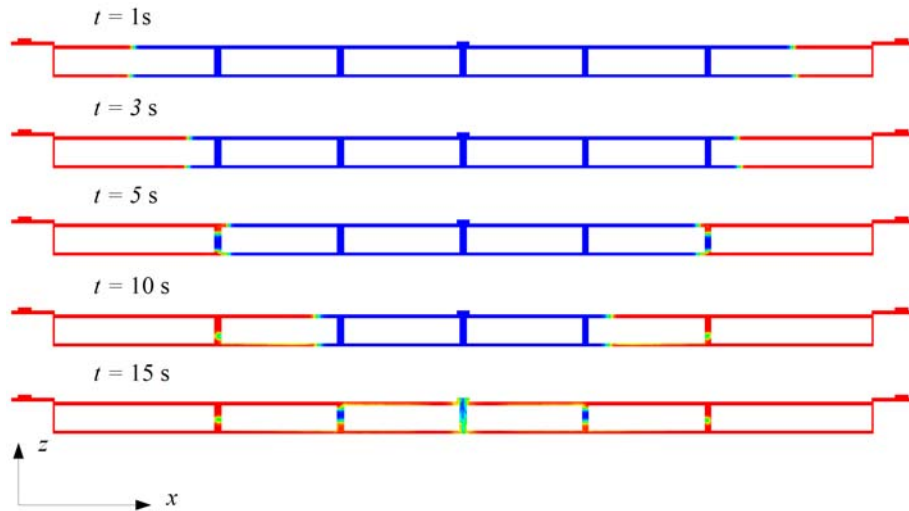


**Figure 6.** Numerical profile infiltration for different filling times cut.

In Figure 7, the region next to the outlet section is amplified. It shows that the injection should last longer than 15s to ensure that all regions are completely filled with resin, however current simulation predicts that the air bubbles entrapped in the connecting tubes will start moving, producing a final piece with undesired void regions (see orange parts in Figure 7).

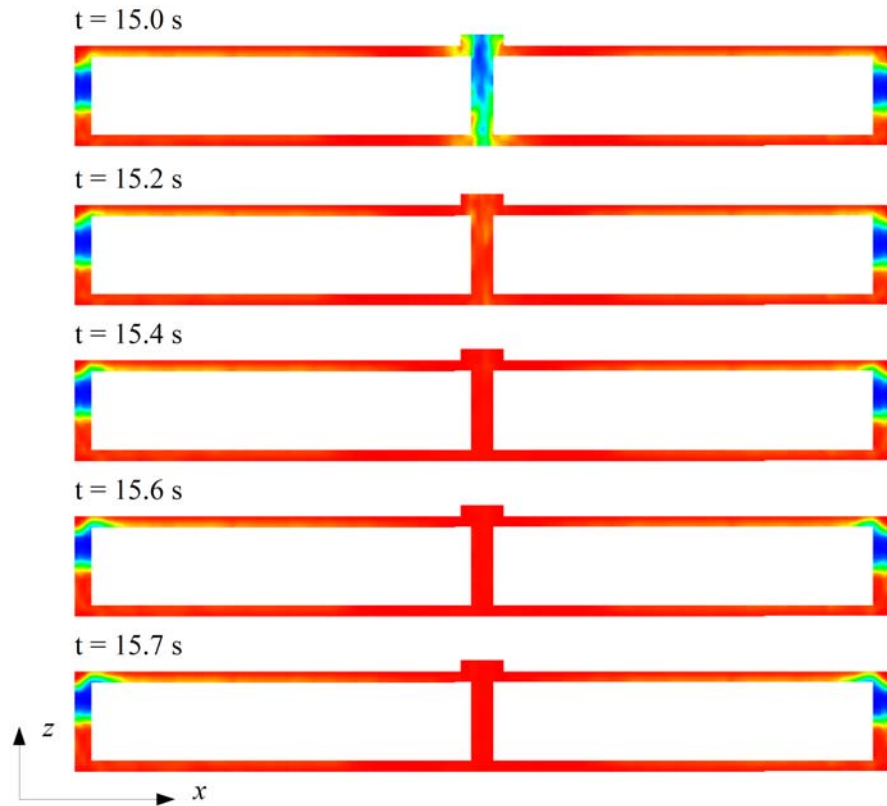


**Figure 7.** Numerical profile infiltration for different filling times cut detail.

In a following experiment, it was investigated what would happen if a second outlet were positioned at the lower sheet. In this case, the connecting tubes are not necessary because the air in the lower sheet will leave the mold by this second outlet. It was expected a decrease in the total filling time however this behaviour has not been observed. The only advantage in including the second outlet was related with the air bubbles formation, which did not appear in this simulation. In Figure 8, calculated resin profiles for different times are shown.

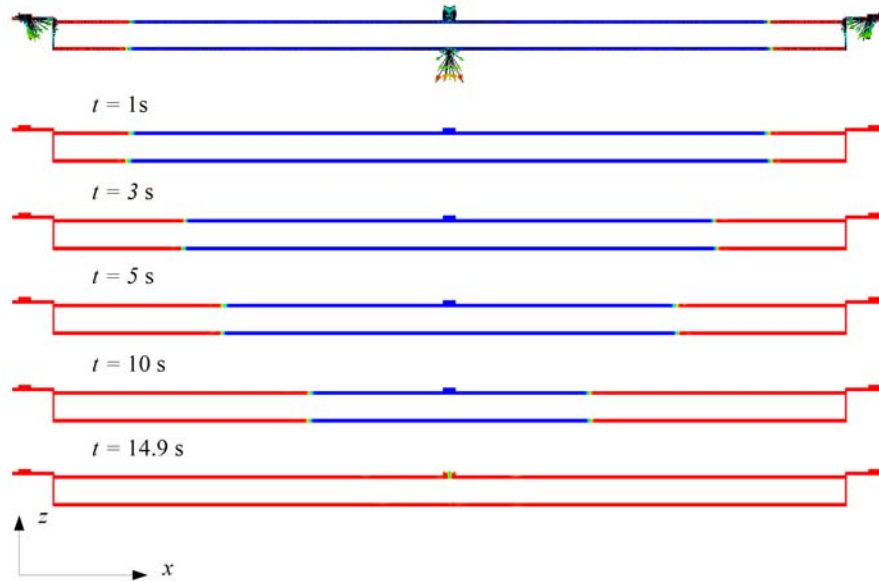


**Figure 8.** Numerical profile infiltration for different filling times - two outlets.

In the last case-study simulated, both the lower outlet and the connection tubes were removed. The idea was to simulate an “extreme” case, with a predictable mold design error, on which a large area without resin impregnation was expected to occur in the lower sheet. The predicted air bubble is shown in Figure 9. As can be seen in this figure, resin starts to advance normally inside the mold in the first few seconds and then the air in the lower sheet becomes entrapped forming an undesired void zone.



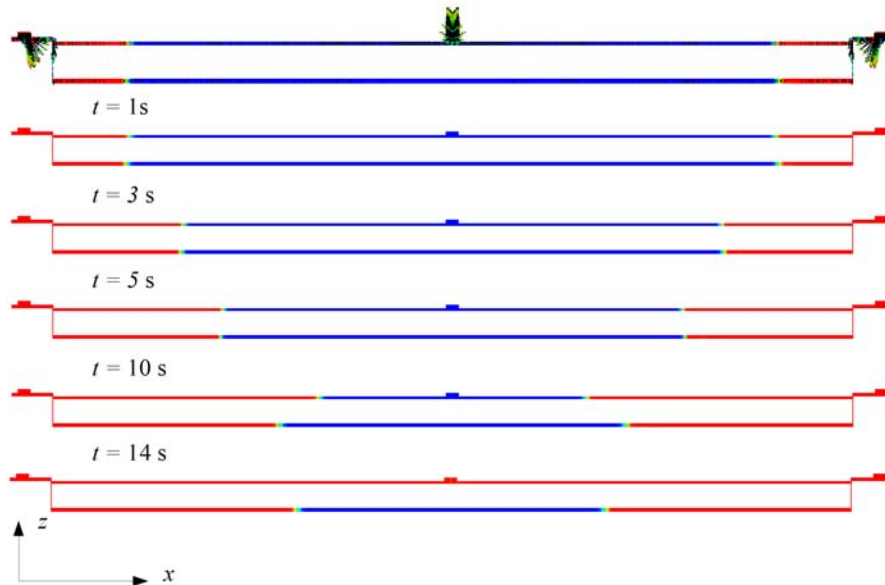


**Figure 9.** Numerical profile infiltration for different filling times - one outlet and no connection tubes.

#### 4. Conclusion

In this work, the VOF method has been used to simulate resin injection in a sandwich composite piece fabricated with the LRTM process. Numerical and experimental runs were compared in terms of filling time and flow profiles inside the mold cavity. Results have confirmed that it is possible to predict flow advance and void formation in RTM composites using numerical techniques.

Three case-studies were run. The first one was used to validate the numerical solution. It was compared with an experimental run. Filling time agreed within 18% difference and resin flow front comparison showed similar profiles. These results were considered good because the irregular geometry of the injection channel could not be precisely drawn (computational domain) and media permeability was estimated in a different experiment.

The second case-study modifies the experiment run and investigates the viability of reducing filling time with the addition of a second outlet to the lower section of the mold. As was explained, numerical run showed that filling time is almost identical in both cases.

In the third and last case-study, the first run, with only one outlet, was simulated again, however this time the connection tubes used to facilitate air to escape from the lower sheet were removed. In this case, as expected, it was numerical predicted that a large amount of air would be entrapped at the lower part of the mold.

### Acknowledgements

The author acknowledges the Conselho Nacional de Desenvolvimento Científico e Tecnológico (CNPq), the Coordenação de Aperfeiçoamento de Pessoal de Nível Superior (CAPES), and the Fundação de Amparo à Pesquisa do Estado do Rio Grande do Sul (FAPERGS) for the financial support.

### References

- [1] M. V. Brusckhe and S. G. Advani, A finite-element control volume approach to mold filling in anisotropic porous-media, *Polym. Compos.* 11(6) (1990), 398-405.
- [2] J. A. Luoma and V. R. Voller, An explicit scheme for tracking the filling front during polymer mold filling, *Appl. Math. Model.* 24(8-9) (2000), 575-590.
- [3] S. G. Advani and E. M. Sozer, *Process Modeling in Composites Manufacturing*, 2nd Edition, CRC Press, Taylor & Francis Group, 2010.
- [4] F. R. Phelan, Simulation of the injection process in resin transfer molding, *Polym. Compos.* 18(4) (1997), 460-476.
- [5] C. W. Hirt and B. D. Nichols, Volume of fluid (VOF) method for the dynamics of free boundaries, *J. Comput. Phys.* 39(1) (1981), 201-225.
- [6] J. Yang, Y. X. Jia, S. Sun, D. J. Ma, T. F. Shi and L. J. An, Enhancements of the simulation method on the edge effect in resin transfer molding processes, *Mater. Sci. Eng. A* 478(1-2) (2008), 384-389.
- [7] J. A. García, L. Gascón and F. Chinesta, A fixed mesh numerical method for modelling the flow in liquid composites moulding processes using a volume of fluid technique, *Comput. Methods Appl. Mech. Eng.* 192(7-8) (2003), 877-893.

- [8] M. Moeini Sedeh and J. M. Khodadadi, Interface behavior and void formation during infiltration of liquids into porous structures, *Int. J. Multiph. Flow* 57 (2013), 49-65.
- [9] J. Bréard, A. Saouab and G. Bouquet, Numerical simulation of void formation in LCM, *Compos. Part Appl. Sci. Manuf.* 34(6) (2003), 517-523.
- [10] E. Ruiz, V. Achim, S. Soukane, F. Trochu and J. Breard, Optimization of injection flow rate to minimize micro/macro-voids formation in resin transfer molded composites, *Compos. Sci. Technol.* 66(3-4) (2006), 475-486.
- [11] J. A. Souza, L. A. Isoldi, E. D. dos Santos, C. P. Oliveira and S. C. Amico, A Numerical Methodology for Permeability Determination of Reinforcements for Polymeric Composites, in *ENCIT 2012 - Book of Abstracts*, Rio de Janeiro, RJ - Brazil (2012), 1-7.
- [12] S. K. Kim and I. M. Daniel, Determination of three-dimensional permeability of fiber preforms by the inverse parameter estimation technique, *Compos. Part Appl. Sci. Manuf.* 34(5) (2003), 421-429.
- [13] O. Restrepo, K.-T. Hsiao, A. Rodriguez and B. Minaie, Development of adaptive injection flow rate and pressure control algorithms for resin transfer molding, *Compos. Part Appl. Sci. Manuf.* 38(6) (2007), 1547-1568.
- [14] S. Laurenzi, A. Casini and D. Pocci, Design and fabrication of a helicopter unitized structure using resin transfer moulding, *Compos. Part Appl. Sci. Manuf.* 67 (2014), 221-232.
- [15] L. A. Isoldi, C. P. Oliveira, Luiz A. O. Rocha, Jeferson A. Souza and S. C. Amico, Three-dimensional numerical modeling of RTM and LRTM processes, *J. Braz. Soc. Mech. Sci. Eng.* 34(2) (2012), 105-111.
- [16] S. H. Han, E. J. Cho, H. C. Lee, K. Jeong and S. S. Kim, Study on high-speed RTM to reduce the impregnation time of carbon/epoxy composites, *Compos. Struct.* 119 (2015), 50-58.
- [17] C. Geuzaine and J.-F. Remacle, Gmsh: A 3-D finite element mesh generator with built-in pre- and post-processing facilities, *Int. J. Numer. Methods Eng.* 79(11) (2009), 1309-1331.
- [18] H. G. Weller, G. Tabor, H. Jasak and C. Fureby, A tensorial approach to computational continuum mechanics using object-oriented techniques, *Comput. Phys.* 12(6) (1998), 620.
- [19] V. Srinivasan, A. J. Salazar and K. Saito, Modeling the disintegration of modulated liquid jets using volume-of-fluid (VOF) methodology, *Appl. Math. Model.* 35(8) (2011), 3710-3730.
- [20] P. Higuera, J. L. Lara and I. J. Losada, Realistic wave generation and active wave absorption for Navier-Stokes models, *Coast. Eng.* 71 (2013), 102-118.

